ISSN 0020-4412, Instruments and Experimental Techniques, 2014, Vol. 57, No. 4, pp. 381–385. © Pleiades Publishing, Ltd., 2014.
Original Russian Text © V.I. Aleinik, D.A. Kasatov, A.N. Makarov, S.Yu. Taskaev, 2014, published in Pribory i Tekhnika Eksperimenta, 2014, No. 4, pp. 9–13.

NUCLEAR EXPERIMENTAL TECHNIQUES

Measuring the Neutron Spectrum of the Accelerator-Based Source Using the Time-of-Flight Method

V. I. Aleinik[a], D. A. Kasatov[b], A. N. Makarov[a], and S. Yu. Taskaev[a]

[a] *Budker Institute of Nuclear Physics, Siberian Branch, Russian Academy of Sciences, pr. Akademika Lavrent'eva 11, Novosibirsk, 630090 Russia*
e-mail: alexxmak314@gmail.com

[b] *Novosibirsk State University, ul. Pirogova 2, Novosibirsk, 630090 Russia*

Received October 10, 2013

Abstract—The time-of-flight technique with a new method for generating short radiation bursts has been used to measure the neutron spectrum of the accelerator-based source with a stationary proton beam. Specific problems arising thereby and methods for solving them are described. The measured spectrum of neutrons in the reaction ^{7}Li(p, n)^{7}Be at a proton energy of 1.915 MeV is presented and compared to the calculation. This spectrum is shown to comply with the requirements for the neutron beam used in neutron capture therapy.

DOI: 10.1134/S0020441214030026

INTRODUCTION

Boron neutron capture therapy (BNCT) is considered today to be a promising technique for treating malignant tumors. BNCT implies selective destruction of tumor cells by preliminary accumulation of stable ^{10}B isotope in them and subsequent neutron irradiation [1]. Absorption of a neutron by a boron nucleus initiates nuclear reaction ^{10}B(n, α)^{7}Li followed by high energy release in a cell, which results in its destruction. Tests performed at nuclear reactors have shown that BNCT allows treatment of brain glioblastoma and melanoma metastases [2, 3]. For wide clinical application of the technique, it is necessary that epithermal neutron sources based on charged particle accelerators be developed. A source based on an electrostatic tandem accelerator with the vacuum insulation of the electrodes and on neutron production reaction ^{7}Li(p, n)^{7}Be was proposed in [4]. A prototype of the accelerator-based epithermal neutron source was constructed, and generation of neutrons was effected in [5]. The neutron yield was measured by the activation of the target with radioactive isotope ^{7}Be, which is necessarily produced in generation of neutrons, and by detection of β^- decay of ^{128}I isotope produced by a neutron flux in the NaI crystal of the γ spectrometer. The epithermal character of the neutron spectrum was qualitatively corroborated by readings of the BDT and BD100R bubble detectors sensitive to neutrons with different energy ranges.

In this paper, we present and discuss the spectra of generated neutrons measured by the time-of-flight (TOF) method in which the neutron energy is determined in a short radiation burst by the delay time of their detection with a remote detector.

The use of the TOF method makes it possible to reconstruct the epithermal neutron spectrum with a high accuracy and reliability.

A new engineering solution has been proposed for generating short neutron bursts. It is based on the threshold character of the cross section for reaction ^{7}Li(p, n)^{7}Be. The solution resembles the well-known blinking-accelerator method. The accelerator operates in the stationary mode at a proton beam energy below the 1.882-MeV threshold of reaction ^{7}Li(p, n)^{7}Be, and neutrons are not generated. After a negative short (200 ns) 40-kV voltage pulse is applied to the neutron-generating target, which is electrically insulated from the setup housing, proton energy increases to 1.915 MeV, which results in a neutron burst. Rectangular-shaped high-voltage pulses are generated using a double shaping line and a thyratron operating by way of a switch with a frequency of 100 Hz. Neutrons are detected by a remote detector composed of a GS20 lithium-containing scintillator 18 mm in diameter and 4 mm thick and a photomultiplier tube. The time of flight (TOF) of a neutron is determined by a ВЦП-1 time-to-digital converter (TDC): the time interval is measured between the instants when a high voltage is applied to the target and the signal from the neutron detector appears. The proposed engineering solution for generation of short neutron bursts, including the circuit diagram of the generator, the measured pulse waveform, the evaluated neutron detection efficiency, and results of calibration using an α–Be source were described in detail in [6].

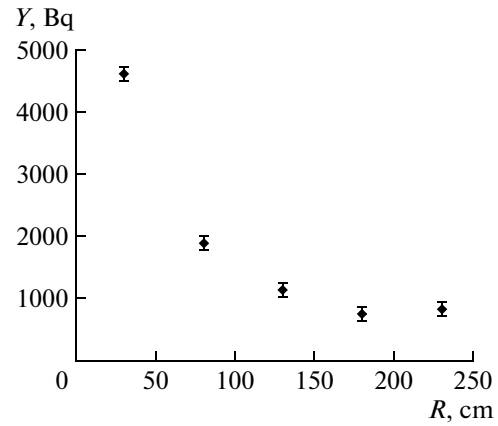

Fig. 1. Dependence of activity Y of ^{115}In pellets on distance R to the target.

PROBLEMS ENCOUNTERED IN NEUTRON SPECTRUM MEASUREMENTS

A number of problems have been encountered when taking neutron spectrum measurements, and their effect has been minimized where possible.

The first problem was associated with the electromagnetic noise induced by generated short high-voltage pulses in the measuring equipment and accelerator devices. The noise caused malfunctions and false triggering both in the TOF measuring equipment and in the accelerator control circuits, and, moreover, in the high voltage pulse generation circuit. A high-frequency ferrite filter was set at the power supply input of the pulse generation circuit to suppress noise induction, and all assemblies of the high-voltage circuit were grounded through it. Ferrite rings were attached to the accelerator control wires and the high-voltage circuit. The neutron generating target was surrounded by a grounded metal shield. All the measuring equipment near the detector was enclosed in an antijam box with power supply filtering. The neutron detector itself was placed inside a grounded shield, and its wires were also shielded. All these measures have made it possible to generate short high-voltage pulses and make measurements.

The next problem can be attributed to the so-called background neutrons. The point is that the concept of TOF measurements imposes rigid requirements for the background neutron flux level, since measurable neutrons are generated in a short time interval (in our case, 200 ns) and detected for a longer (a factor of 500) time if the accelerator is in operation. The appearance of background neutrons is associated with two factors. First, during transportation, a small fraction of the proton beam hits the stainless steel walls of the vacuum chamber and initiates neutron generation as a result of reaction ^{55}Mn(p, n)^{55}Fe. The manganese content of 12X18H10T steel is known to be 2%. Though the cross section of reaction ^{55}Mn(p, n)^{55}Fe is much smaller than the cross section of reaction ^{7}Li(p, n)^{7}Be, but, at the same time, the reaction threshold is much lower, being only 1.034 MeV. Therefore, interaction between the proton beam halo and the walls of the vacuum pipe initiates generation of a neutron flux, though being small in value, but essentially hindering the taking of measurements. This neutron background was suppressed by shielding the chamber walls with a molybdenum foil along the whole transport beamline. Second, background neutrons can be generated in constructional materials near a target, e.g., in a copper substrate in reaction ^{63}Cu(α, n)^{66}Ga: high-energy α particles are produced in reaction ^{7}Li(p, α)^{4}He when the proton beam passes through the lithium layer.

One more way for suppressing the spurious background neutron signal is associated with neutron reflection from the walls and the floor of a room that houses the setup and the neutron detector. The degree of the effect of reflected neutrons has been estimated from experiments conducted with activation detectors—^{115}In pellets with a diameter of 10.0 mm, a thickness of 0.4 mm, and a mass of 0.2 g. The activity of the ^{115}In pellets is presented in Fig. 1 as a function of the distance from the target until it reached a value of 239 cm at which the pellets were placed on the floor of the protected shelter. It is apparent that the contribution of reflected neutrons to the activation of pellets becomes significant near the floor. To reduce the effect of reflected neutrons, the neutron detector was lifted above the floor to a height of 1.5 m.

The next problem can be attributed to the spurious signal of γ quanta. Though the neutron detector based on a lithium glass is based on reaction $^{6}\mathrm{Li} + n \longrightarrow {}^{3}\mathrm{H} + \alpha + 4.785$ MeV, high-energy γ quanta may also produce as bright scintillations in the lithium glass as neutrons do. Figure 2 presents the γ-ray spectra measured by a BGO spectrometer located at a distance of 160 cm from the target in a lead shielding. The spectra were obtained for two proton energies one of which was below the neutron generation threshold. It is apparent that, apart from the clearly discernible 478-keV peak attributable to the proton–lithium interaction, γ quanta with energies as high as 4.8 MeV and even higher are produced when neutrons are generated. In Fig. 3, it is evident that the detector detects neutrons, which form a clearly discernible peak *1*, as well as γ quanta with a wide spectrum of signal amplitudes *2*. An amplitude discriminator is used to cut off the signals from γ quanta with amplitudes lower than the amplitudes of the characteristic neutron signals. A lead shielding 7 cm thick is used to attenuate the high-energy photon flux producing the signals indistinguishable from the neutron signals. The shielding allows the photon flux with energies of a few MeV to be reduced by a factor of 100 [7]. In this case, the lead shielding does not affect the neutron spectrum shape, since the cross section for neutron scattering from lead is almost constant at neutron energies ranging from 1 eV to 100 keV.

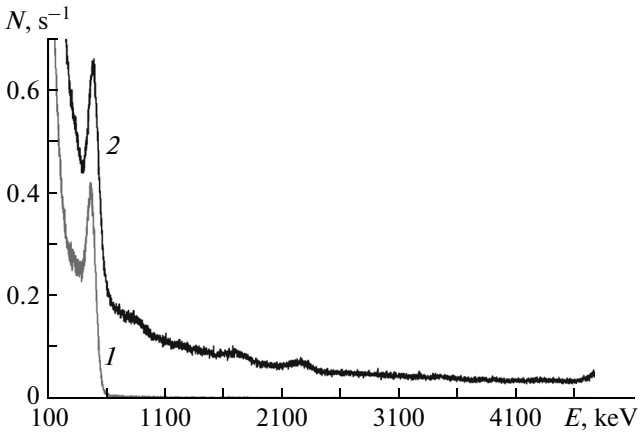

Fig. 2. Spectrum of γ quanta from the neutron-generating target upon incidence of the proton beam with energies of (*1*) 1.870 and (*2*) 1.930 MeV on it: (*N*) counting rate.

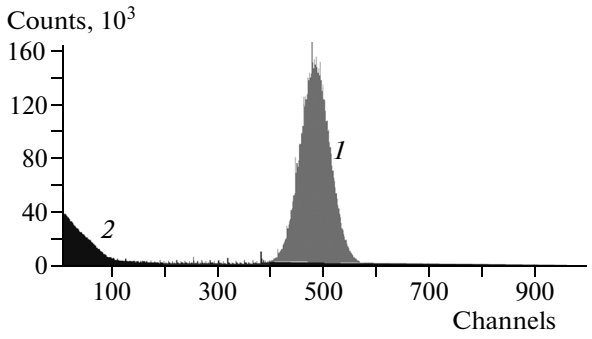

Fig. 3. Characteristic spectrum of the neutron detector signals: (*1*) neutron bursts and (*2*) noise due to high-energy γ quanta.

One more difficulty is caused by the instability of the accelerator voltage. Though the electrostatic tandem accelerator ensures a high stability of the proton beam energy (10 keV), nevertheless, this stability is critical for the TOF method. To avoid unplanned neutron radiation bursts, the proton energy was decreased by 10 keV below the reaction threshold. However, this could not always help us, since the proton energy instability sometimes reached a value of 20 keV. Each neutron burst originated by a proton energy jump may be responsible for as many as 1000 and even more noise events in the spectrum being measured at that time, wasting thereby several hours of data acquisition. Program filtering was used to eliminate this background. It monitored the accelerator voltage in a real time mode and acquired the neutron spectrum data. If the accelerator voltage fell beyond the predetermined limits (Fig. 4), data acquisition was halted, and, when the voltage recovered, was automatically resumed. The use of this program has made it possible to closer approach the neutron production threshold (up to 1875 ± 5 keV) and to reject background spikes. As a result, the neutron spectrum was measured at a proton energy of 1915 ± 5 keV. Apart from the pulse character of the accelerator voltage instability, additional slow variation in the voltage was observed and corrected manually.

One more difficulty in taking TOF measurements consisted in the absence of routine diagnostics of the beam at the target. Since high voltage pulses were applied to the target, it was impossible to use the current, calorimetric, and dosimetric diagnostics. The temperature method remained the sole method for monitoring the beam position near the target. The beam displacement could be measured by means of four thermocouples fixed in place on the sides of the vacuum chamber near the target. Nevertheless, this method fails to be precise and fast and is better suitable as a protective means against possible vacuum section burning-through caused by the beam. Therefore, it was proposed using the following method for additional diagnostics. The interval in which neutrons are detected by means of the ВЦП-1 TDC is 100 μs. In addition, when the neutron detector was placed at a distance of 78 cm, neutrons with energies ranging from 2 eV to 200 keV were detected in the first 50 μs, and slower neutrons were measured in the next 50 μs. Abandoning detection of slow neutrons, it is possible to measure the noise level due to random events. To do this, it is sufficient that acquisition of neutron events by the ВЦП-1 TDC start 50 μs earlier than the application of a high voltage pulse initiating a neutron burst. The neutron detector measures only the noise signal until a neutron burst happens and, after the burst, the useful signal as well. The use of this method in the neutron spectrum acquisition is illustrated in Fig. 5. Therefore, at any instant of time, it is possible to monitor the actual signal-to-noise ratio. Deterioration of this ratio means that the beam position and/or energy must be corrected.

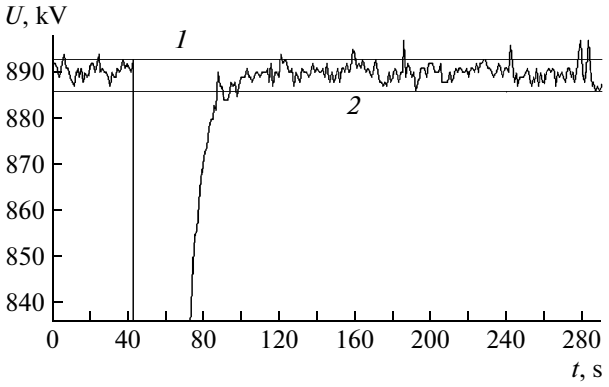

Fig. 4. Example of the filtering program operation in the course of the TOF experiment: (*U*) accelerator voltage, (*t*) time, and (*1*) upper and (*2*) lower limits of the voltage.

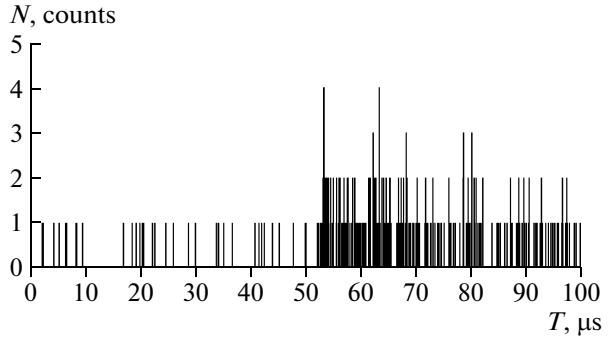

Fig. 5. Data acquisition process during the experiment of March 7, 2013: (*T*) flight time and (*N*) counts. Only noise events are shown in the first 50 μs, and the signal + noise values are presented in the subsequent 50 μs.

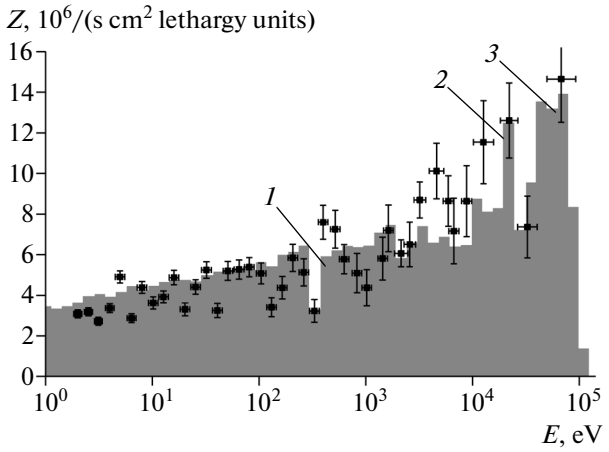

Fig. 6. Measured neutron spectrum: columns present the calculated neutron spectrum, dots show the measured spectrum, and the characteristic features of the spectrum are labeled by numbers *1–3*.

RESULTS OF MEASUREMENTS AND DISCUSSION

The neutron spectra measured using the TOF method over 5 days are shown in Fig. 6 in comparison with the calculated neutron spectrum [8].

For the neutron energy to be determined, both the measured TOF and the path lengths of neutrons must be known. If a mechanical chopper placed behind the target is used to produce short neutron bursts, the path length would be unambiguously defined by the chopper-to-detector distance. In our case of application of the blinking accelerator method, the situation is worse. Neutrons generated in a thin lithium layer pass thereafter through the target assembly proving efficient heat pickup. The target assembly with a thickness of 6 cm is made of stainless steel and has water supply channels with a characteristic size as large as 2.2 cm [9]. Passing of neutrons through the target assembly is followed by their scattering and moderation by elastic scattering in the water. Thus, for example, the neutron energy decreases over five collisions from the initial value of 40 keV (the mean energy of emitted neutrons) to 300 eV. Since the neutron range characteristic of these energies in water is 1.1 cm, a neutron is displaced in five collisions in the initial direction for a distance of ~1 cm, traveling a path of 5.5 cm. Therefore, the paths that neutrons travel before reaching the detector differ: fast neutrons that do not practically slow down and do not scatter travel a shorter path than those being moderated.

The measured spectrum is shown in Fig. 6 for the case when the neutron path length is assumed to be 84 cm, whereas the distance from the center of the lithium layer in the target to the detector end surface is 78 cm. The selection of this distance is explained by the desire to match the clearly discernible dip in the neutron flux at energies of 300–400 eV both in the calculated spectrum (316–398 eV) and in the measured distribution (*1* in Fig. 6). This dip can be attributed to neutron scattering from ^{55}Mn nuclei that are present in the stainless steel in an amount of 2%. In this energy range, the cross section of neutron scattering from ^{55}Mn nuclei has a wide peak with a maximum of 3232 b at an energy of 340 eV.

Peaks *2* and *3* in the neutron spectrum in Fig. 6 are due to the free flight of neutrons through iron, since the cross section of neutron scattering from ^{55}Fe nuclei at energies of 24.5, 72.9, and 82.0 keV is by three orders of magnitude smaller than the characteristic scattering cross sections in this energy range. It is apparent that the measured spectrum complies with the theoretical one. However, the best agreement in this energy range is observed when the flight path is assumed to be 80 instead of 84 cm. If we take into account that the GS20 glass is located at some distance from the detector end surface and that neutrons are generated on a surface 10 cm in diameter, the obtained fast-neutron path length of 80 cm is in good agreement with the distance from the center of the lithium target to the detector end surface, which is 78 cm. We also notice that the experimentally determined 4-cm difference in the path lengths of neutrons with energies of 40 keV and 300 eV is explained well by the scattering of the latter neutrons in water.

As a result, the neutron spectrum corroborating the theoretical data has been measured at the accelerator-based neutron source using the TOF technique. The produced neutron flux with a mean energy of 13 keV corresponds to the "ideal" neutron spectrum for BNCT [10, 11].

CONCLUSIONS

The epithermal neutron source based both on the electrostatic tandem accelerator with the vacuum insulation of the electrodes and on generation of neutrons in threshold reaction ^{7}Li(p, n)^{7}Be has been designed with the aim of developing a technique for

neutron capture therapy of malignant tumors. The TOF diagnostic complex has been developed to measure the neutron spectrum using the TOF method, and neutron generation has been performed based on the new engineering solution.

The engineering solutions allowing us to minimize the influence of electromagnetic noise pickup, spurious neutrons, high-energy γ quanta, and the accelerator voltage instability on measurements of the generated neutron flux spectrum have been presented in the paper. Data acquisition over 5 days has made it possible to reconstruct the neutron spectrum with a high degree of detail. The measured neutron spectrum complies with the theoretical spectrum with a high degree of accuracy, including details due to moderation of neutrons and their resonant scattering or transmission. It has been experimentally confirmed that the spectrum of the generated neutron flux complies with the ideal spectrum required for neutron capture therapy.

ACKNOWLEDGMENTS

This work was supported in part by the Ministry of Education and Science of the Russian Federation, state contract no. 14.512.11.0105 of July 8, 2013.

REFERENCES

1. Locher, G. and Roentgenol, A.J., *Radium Ther.*, 1936, vol. 36, p. 1.
2. Hatanaka, H., *Basic Life Sci.*, 1990, vol. 54, p. 15.
3. Hatanaka, H. and Nakagawa, Y., *Int. J. Radiat. Oncol. Biol. Phys.*, 1994, vol. 28, p. 1061.
4. Bayanov, B., Belov, V., Bender, E., Bokhovko, M., Dimov, G., Kononov, V., Kononov, O., Kuksanov, N., Palchikov, V., Pivovarov, V., Salimov, R., Silvestrov, G., Skrinsky, A., Soloviov, N., and Taskaev, S., *Nucl. Instrum. Methods Phys. Res., A*, 1998, vol. 413, p. 397. DOI: 10.1016/S0168-9002(98)00425-2
5. Kuznetsov, A.S., Malyshkin, G.N., Makarov, A.N., Sorokin, I.N., Sulyaev, Yu.S., and Taskaev, S.Yu., *Tech. Phys. Lett.*, 2009, vol. 35, p. 346.
6. Aleynik, V., Bayanov, B., Burdakov, A., Makarov, A., Sinitskiy, S., and Taskaev, S., *Appl. Rad. Isotopes,* 2011, vol. 69, p. 1639. DOI: 10.1016/j.apradiso.2011.02.014
7. Mashkovich, V.P., *Zashchita ot ioniziruyushchikh izluchenii: Spravochnik* (Protection from Ionizing Radiations: A Handbook), Moscow: Energoatomizdat, 1982.
8. Bayanov, B., Kashaeva, E., Makarov, A., Malyshkin, G., Samarin, S., and Taskaev, S., *Appl. Rad. Isotopes*, 2009, vol. 67, Suppl. 1, p. 282. DOI: 10.1016/j.apradiso.2009.03.076
9. Bayanov, B., Belov, V., and Taskaev, S., *J. Phys.*, 2006, vol. 41, p. 460.
10. Kreiner, A., *Neutron Capture Therapy. Principles and Applications*, Sauerwein, W., Wittig, A., Moss, R., and Nakagawa, Y., Eds., Heidelberg: Springer-Verlag, 2012, p. 43. DOI: 10.1007/978-3-642-31334-9
11. Leung, K., *Neutron Capture Therapy. Principles and Applications*, Sauerwein, W., Wittig, A., Moss, R., and Nakagawa, Y., Eds., Heidelberg: Springer-Verlag, 2012, p. 65. DOI: 10.1007/978-3-642-31334-9

Translated by N. Goryacheva